JOURNAL OF NANOSCOPE
ISSN(P): 2707-711X | ISSN(O): 2788-7456 *Volume 2, Issue 1, June 2021, pp 29-38*

Effect of Reduced Dimensionality on the Magnetic and Transport Properties of Ca Doped Colossal Magnetoresistive Nanoparticles

S. Qaseem[1], M. Naeem[2 *], M. Ikram[3], Nimra Niamat[4]
[1]Department of Physics, Federal Urdu University of Arts, Science and Technology Karachi Pakistan.
[2]Department of Physics, University of Karachi, Pakistan.
[3]Department of Physics, Hazara University, Mansehra 21300, Pakistan.
[4]Government Degree College for Women, Lodhran, Pakistan.
Corresponding Author: naeem.khan@uok.edu.pk

Received: 03 March 2021 **Published:** 30 June 2021

Abstract
Magnetic and electrical measurements of different nanosize Ca doped colossal magnetoresistive $La_{0.7}Ca_{0.3}MnO_3$ are reported. The nanoparticles are synthesized with the modified citrate rout at different temperatures. X-ray diffraction measurements revealed three dominant peaks 23.04^0, 40.517^0 .47.17^0, 58.66^0 which confirms the perovskite-like structure. The average crystallite size the nanoparticles are found to be 20 to 32nm. All the synthesized nanoparticles exhibit ferromagnetic ordering close to the phase transition temperatures. The size dependent magnetic and electrical transport properties are explored at different fields and temperature. Saturation magnetization is found to decrease with decreasing particle diameter. It is found that the particle size can tune the trend of coercive field. Coercive field first increases from 78 to 210 Oe and then decreases to 174 Oe. The electrical transition temperature is found to be 158 K for 20nm particle. Oxygen deficiency in such system generally reduces Mn^{4+} to Mn^{3+} to keep the charge neutrality of the structure and hence it destroys the conduction path ways to mobile electrons, at least in long range, and thus insulating behavior becomes more prominent in the larger temperature range. The trend at lower temperature attribute to the coulomb blockade.

Keywords
Conduction, electrons, temperature, nanoparticles and magnetic.

DOI Number: *10.52700/jn.v2i1.26*

INTRODUCTION:

Ca-doped $LaMnO_3$ CMR perovskite is one of the potential candidates in data storage devices, fuel cell electrodes and highly sensitive magnetic sensors [1]. Verity of preparation methods has been adopted to synthesize Ca doped CMR NPs, which is important not only for manufacturing electrodes and magnetic sensors, but also to understand the CMR phenomenon. Many researchers explored the size dependent properties of CMR NPs but there are conflicting results reported in literatures. Arun et al. reported [2] the formation of disorders over the surface increases which leads to the physical properties, such as magnetic and electrical behaviours, strongly depend on the particle size. The transition temperature was reported, by Hintze et al., significantly reduced to 22% as size of the particle reduces to 26 nm. Dey and Nath [4] found that ferromagnetic transition temperature does not vary with particle size but metal-insulator transition temperature depends on the particle size. They used spin polarized tunneling model for their results. Similarly, Lopez-Quintela *et al.* [5] also reported constant T_c for the range of 60 - 500 nm particles. They also mentioned that saturation magnetization decreases with the particle size which supports the core shell model for nanoparticles. Whereas various research groups [6] reported decrease in T_C with increasing particle size. They referred the work of Dutta et al. [7] where the increase in particle size increases of Mn-O-Mn bond length and decrease of the bond angle, which decreased T_C. However, another study by Siwach et al. [8] have shown increase in Tc and T_m with particle size. So there are some conflicting results published on the same compound $La_{0.7}Ca_{0.30.3}MnO_3$.

In this paper, we report the detail sample preparation and characterization. The main objective is to address the behavior of magnetic and electrical transport properties by reducing particle size. Subsequently many other unexpected effects may appear as a consequence of the particle size reduction. Furthermore, the CMR may have different phases with the variation of dopant concentration such as antiferromagnetic insulators, ferromagnetic metals, canted antiferromagnetic, charge ordering etc. In this research, we focus only x = 3 as it is a ferromagnetic metal [9].

METHOD AND MATERIALS:

The CMR nanoparticles were synthesized via modified citrate route details are given in ref [10]. A drop-wise addition of ethanol into the hydrated citrate solution causes a quic precipitation of narrow distribution nanoparticles. We used lanthanum nitrate, manganese nitrate, calcium chloride, concentrated NH_4OH and citric acid (sigma 99.9%) for synthesis of nanoparticles. First of all, specific composition of initial chemicals was added in citric acid solution with mild stirring and for maintaining the pH to 7 and then added NH_4OH along with the heating at 100 ^oC for two hours. The final solution was extracted by coolant and ethanol was then added dropwise. The precipitation was extracted by miro filter and dried at 120 ^oC. the prepared nanoparticles will be be annealed at three different temperatures, viz 600, 700 and at 800 ^oC and named as LCMO-600, LCMO-700 and LCM)-800 respectively. The structure of the prepared samples were investigated x-ray diffractometer. The crystallite size is estimated by applying the Scherrer's equation.

RESULTS AND DISCUSION:

Structures of the samples were confirmed through X-ray diffraction pattern. Comparing to the XRD data file (PCPDFWIN), we found these peaks match those for the compound of the same composition, i.e $La_{0.7}Ca_{0.3}MnO_3$. The standard peak position in this software is reported as 23.04^0, 40.517^0 .47.17^0, 58.66^0. The intensity comparison of three x-ray patterns is shown in Figure 1 which shows that the crystallization increases with increasing annealing temperature. Sizes of the nanoparticle have been estimated by Scherrer's formula through x-ray diffraction, using single line profile. Theses sizes are found to be 20, 26 and 32 nm for samples LCMO-600, LCMO-700 and LCMO-800 respectively. Magnetization of nanoparticles has been calculated from the vibrating sample magnetometer model BHV-50 of Riken Denish company Ltd. Japan. The measurements of magnetization with applied magnetic fields M(H)-Loops taken at 77 K and at a field of 5 kOe. It is found that the saturation magnetization increases as increasing particle size as shown in the Figure 2. This increasing trend can be understood by considering the core-shell model of nanoparticles. The shell of nanoparticles has lots of defects having no net alignment of magnetic moment and it also hinders the interaction between the neighboring cores of the particles. The lower size particle has high surface defects, which leads to decreases magnetization with the

decreasing particle size. The similar feature has also reported by other groups [5]. The thickness of the surface layer is determined by the formula reported in [11]

$$T = \left[D/2\left\{1 - (M_s/M_{SO})^{1/3}\right\}\right]$$

Where M_s and M_{so} are the saturation magnetization of the bulk sample (M_{so}=74.53emu/gm) respectively. The shell thicknesses are found to be 0.63, 1.37 and 1.24nm for 32, 26 and 20 nm sizes respectively. Coercivity behavior is also shown in Figure 2. It can be seen from figure, first coercivity increases with decreasing particle size from 176 Oe to 210 Oe and then it decreases to 76 Oe for 20nm size particle. In order to explain this behavior of coercivity, we use the domain criterion. Larger size particles may have domains thus magnetization reversal is dominated by domain wall motion, which is relatively easy, hence the coercivity is low. However, for decreasing particle size, the coercivity is found to follow empirical relationship [12] until the single domain size is reached

$$H_C = a + b/D$$

The largest coercivity occurs at the single domain size. Below this, Hc falls of due to thermal activation over the anisotropy barriers and leading to superparamagnetism for which H_c=0 Oe. In our case, the coercivity of the smallest size particle is found to be 78 Oe which could be due to the broad size distribution of nanoparticles. The critical size for single domain particle of this particular compound has not been reported yet but it lies in the range of 26 nm to 32 nm according to our results. A.C Susceptibility measurements were conducted using a self made A.C probe with a split secondary (astatically wound) and a commercially lock in amplifier. The sample could be moved between two secondary coils which enable a careful cancellation of the background. The measurements were taken at A.C field of $H_{a.c}$ = 10 Oe at a constant frequency of 573 Hz on all samples. A.C susceptibility curves for samples LCMO-600, LCMO-700 and LCMO-800 are shown in Figure 3(a), (b) and (c). All spectra show both the in-phase and out of phase part of susceptibility. Comparison of in phase susceptibility part for all three samples shows that in the smallest particle there is a gradual increase of susceptibility where is for larger particles this is not so which is supposed to be due to the spin blocking at lower temperatures at the surface of the small nanoparticles. The main feature of the out of phase susceptibility curves is that the A.C losses

in all three samples at lower temperature has no difference and it might be due to the intrinsic effects where the difference become prominent at higher temperatures. Furthermore, the paramagnetic curie temperature is determined by plotting $1/\chi$ as a function of temperature. The Curie temperatures are found to be 267 K for 20 nm particle and 270 K for both 26 and 32 nm particles.

In order to measure the electrical resistivity of the sample we use four probe methods. The nanoparticles were first pelletized and sintered at 600^{o} C again for 3 hrs. Figure 4 shows the resistivity behavior of the 20 nm size particles, which is observed during cooling in the presence of applied field of 4.7 k Oe. Figure shows the resistivity behavior when magnetic field is applied parallel and transverse to the pellet. The electrical transition temperature "T_p" is found to be 158 K. This T_p is very low as compared to the magnetic transition temperature (T_c=240 K) reported earlier [13]. The similar drastic change in the electrical and magnetic transition temperature is also found by others [14]. It is reported in literature that the T_p can be affected by different oxygen stoichiometry [2]. In general, the T_p decreases with decreasing oxygen content. We understand this decreasing as follows: Oxygen deficiency in CMR system generally reduces Mn^{4+} to Mn^{3+} to keep the charge neutrality of the structure. Furthermore, oxygen deficiency destroys the conduction path ways to mobile electrons, at least in long range, and thus insulating behavior becomes more prominent in the larger temperature range. The relative resistivity behavior at zero field cooled and field cooled at different fields were also measured as shown in Figure 5(a). For more clarity, temperature dependence of the lnρ as a function of $1/T^{-0.5}$ has been plotted. At lower temperature (> 35 K) range, the lnρ can be fitted with linear fit (shown in the inset of Figure 5(b)), which is a typical behavior of intergranular tunneling associated with a coulomb gap. At lower temperature, thermal energy is not enough to overcome the barrier and hence resistivity starts increasing with decreasing temperature known as coulomb blockade. A granular metal consists of small grains surrounded by insulating material. Usually the values of both grain diameter as well as grain separation follow a broad distribution.

CONCLUSION:

We have observed the effect of size variation on magnetic and electrical properties. Nearly all of our results support the model of core-shell structure. According to the core-shell model nanoparticles has a core in which magnetic moments are regularly aligned and a shell in which moments are not regularly aligned due to the presence of defects. Our results show a decrease in the saturation magnetization with particle size. The interaction between different core spins reduces and hence the magnetization reduces. Moreover A.C susceptibility measurements show that surface transit gradually from disordered to paramagnetic state and shows gradual transition temperature which further supports the surface contribution. Transport properties shows clear dependence of resistivity on magnetic field which is the main feature of a CMR compound further followed by the coulomb blockage at the lower temperature range. This was explained by the weak linkage between the particles caused by surface defects.

.**REFERENCES**

Mishra, D.; Roul, B.; Singh, S.; Srinivasu, V. Possible observation of Griffith phase over large temperature range in plasma sintered $La0.67Ca_{0.33}MnO_3$. J. Magn. Magn. Mater. 2018, 448, 287–291.

Arun, B.; Suneesh, M.V.; Vasundhara, M. Comparative study of magnetic ordering and electrical transport in bulk and nanograined Nd0.67Sr0.33MnO3 manganites. J. Magn. Magn. Mater. 2016, 418, 265–272

Hintze, C.E.; Fuchs, D.; Merz, M.; Amari, H.; Kübel, C.; Huang, M.-J.; Powell, A.; v. Löhneysen, H. Size-induced changes of structural and ferromagnetic properties in La1−xSrxMnO3 nanoparticles. J. Appl. Phys. 2017, 121, 214303

Dey P and Nath TK. Effect of grain size modulation on the magneto- and electronic-transport properties of $La_{0.7}Ca_{0.3}MnO_3$ nanoparticles: The role of spin-polarized tunneling at the enhanced grain surface. Phys. Rev. B 2006; 73: 214425

Lopez-Quintela MA, Hueso LE, Rivas J, Rivadulla F. Intergranular magnetoresistance in nanomanganites, Nanotechnology 2003; 14: 212

Shankar KS, Kar S, Subbanna GN, Raychaudhuri. Enhanced ferromagnetic transition temperature in nanocrystalline lanthanum calcium manganese oxide ($La_{0.67}Ca_{0.33}MnO_3$). Solid State Commun. 2004; 129: 479

Nisar M, Umbreen M, Rafique S, Liaqat B, Batool K, Shahzadi I, Zahra Y, Batool H. Optical Properties of ZnS and Effect of Doping with Transition Elements. JOURNAL OF NANOSCOPE (JN). 2020 Jun 22;1(01):21-33.

Siwach PK, Goutam UK, SrivastavaP, Singh HK, Tiwari RS, Srivastava ON. Colossal magnetoresistance study in nanophasic La0.7Ca0.3MnO3 manganite. J. Phys. D Appl. Phys. 2006; 39:14

Zererak N, un Nisa F, Liaqat B, Kousar F. First Principle's Prediction of the Electronic and Optical properties of Ca4Bi6O13. JOURNAL OF NANOSCOPE (JN). 2020 Jun 22;1(01):35-43

Sankaranarayanan VK, Punkhurst QA, Dickson DPE, Johnson C. Ultrafine particles of barium ferrite from a citrate precursor. J.Magn. and Magn. Materials. 1993; 73 :120

Munir N, Liaqat B, Batool K, Shafiq R, Akhter N, Sattar M, Tariq K. Experimental investigation of low dimensional spin system in metal oxides. JOURNAL OF NANOSCOPE (JN). 2020 Jan 31;1(01)

Kenneth J.Klabunde, Nanoscale materials in chemistry 2001 John Wiley and Sons

Qaseem Q, Maaz K, Mumtaz A and Hasanain SK. Particle size effect on magnetic and transport properties of $La_{0.7}Ca_{0.3}MnO_3$ nanoparticles. The Nucleus 2010; 47: 137-142

Yi T, Gao S, Qi X, Zhu YF, Cheng F, Ma B, Huang Y, Liao C, Yan C. Low temperature synthesis and magnetism of $La_{0.75}Ca_{0.25}MnO_3$ nanoparticles

J. Phys and Chem. of Solids. 2000; 61: 1407

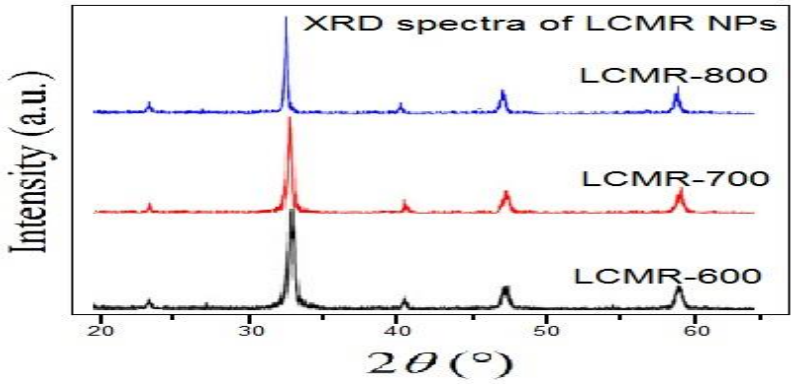

Figure 1: X-ray diffraction patterns of LCMO-600, LCMO-700 and LCMO-800 nanoparticles

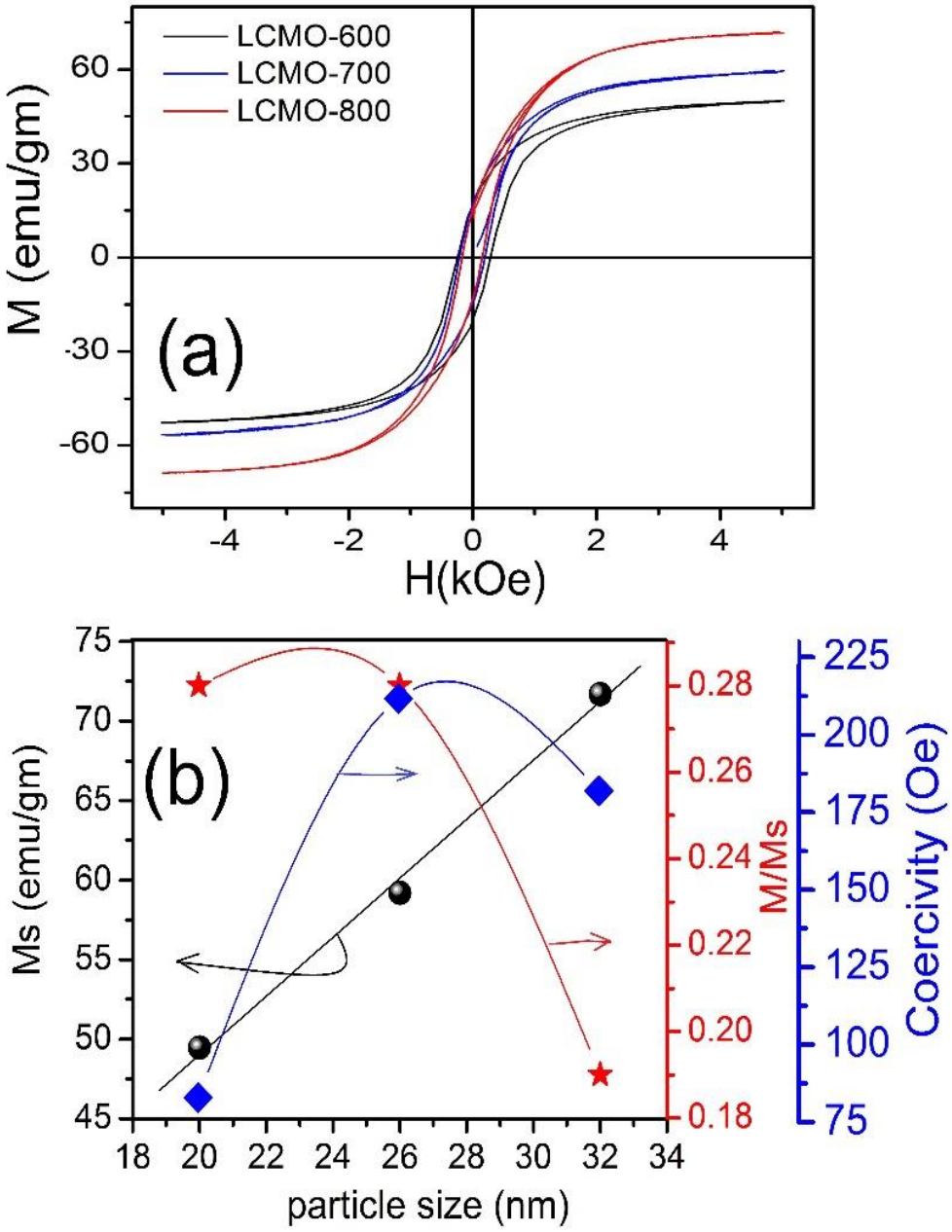

Figure 2: (a) Field dependent magnetization loops of LCMO-600, LCMO-700 and LCMO-800 nanoparticles **(b)** variation of saturation magnetization, Relative saturation magnetization and Coercivity values with respect to particle sizes.

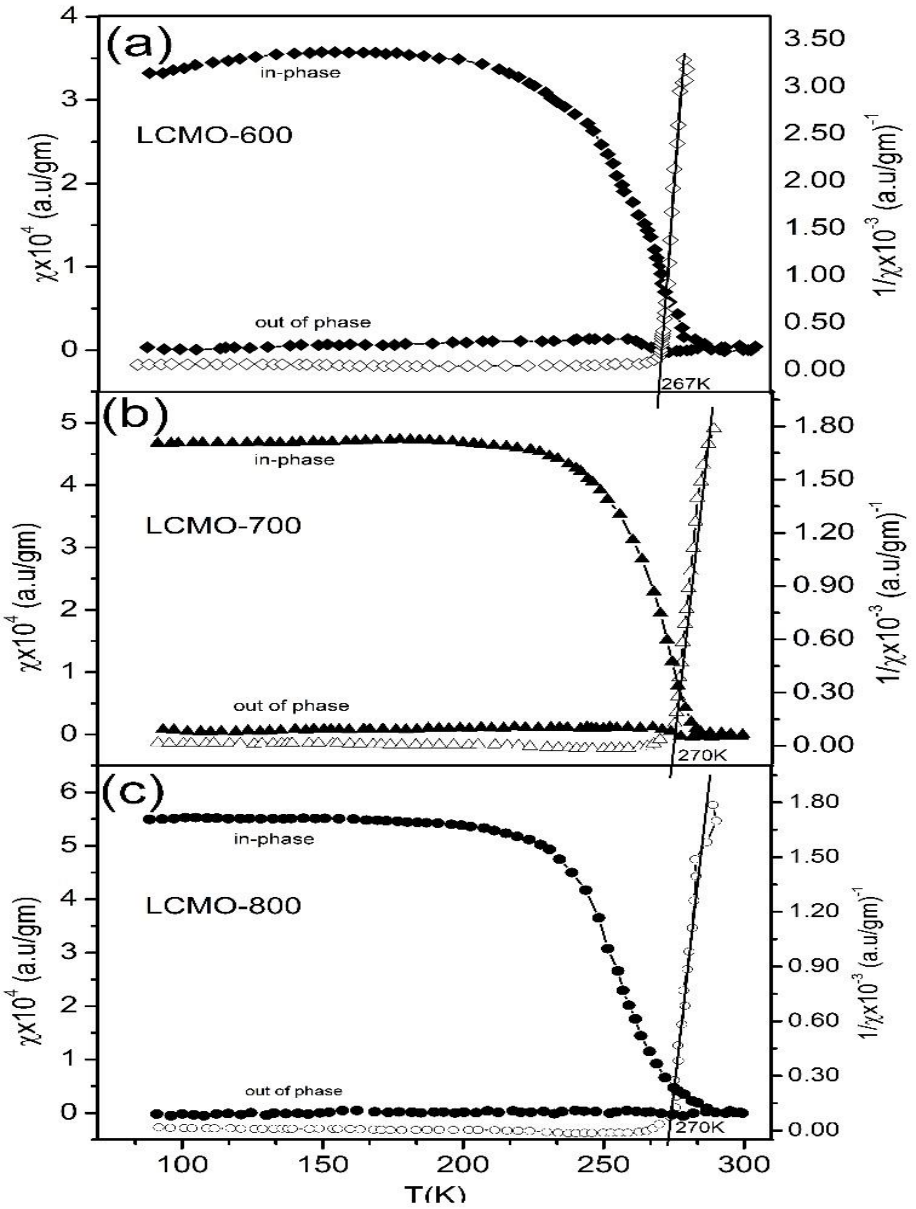

Figure 3: Temperature dependent of AC susceptibility and it inverse plot of LCMO-600, LCMO-700 and LCMO-800 nanoparticles

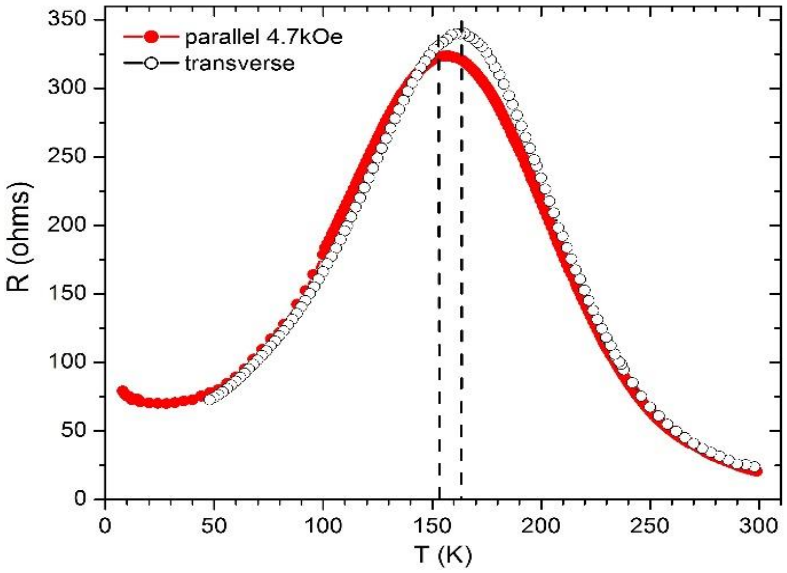

Figure 4: Field dependent of parallel and transverse resistivity plot

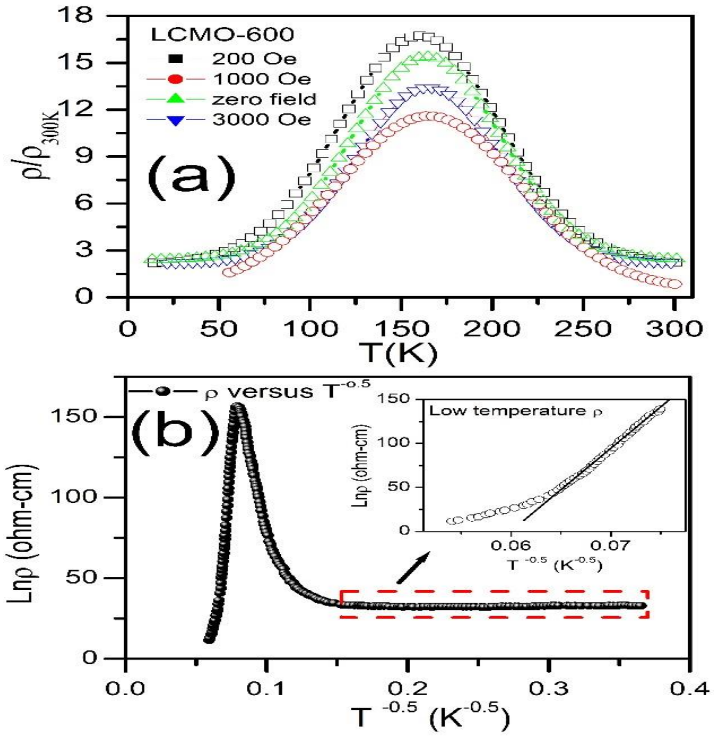

Figure 5: (a) Plot of relative resistivity of field cool and zero field cool of LCMO-600 nanoparticles (b) Low temperature fitting to address the column blockade effect (See detail in text)